



ANNUAL  
REVIEWS **Further**

Click [here](#) to view this article's online features:

- Download figures as PPT slides
- Navigate linked references
- Download citations
- Explore related articles
- Search keywords

# Evolution of Concepts and Technologies in Ophthalmic Laser Therapy

Daniel Palanker

Department of Ophthalmology and Hansen Experimental Physics Laboratory, Stanford University, Stanford, California 94305; email: palanker@stanford.edu

Annu. Rev. Vis. Sci. 2016. 2:295–319

The *Annual Review of Vision Science* is online at [vision.annualreviews.org](http://vision.annualreviews.org)

This article's doi:

10.1146/annurev-vision-111815-114358

Copyright © 2016 by Annual Reviews.

All rights reserved

## Keywords

laser, laser–tissue interactions, retinal laser therapy, ultrafast laser surgery, refractive surgery

## Abstract

Ophthalmology was the first medical specialty to adopt lasers right after their invention more than 50 years ago, and they gradually revolutionized ocular imaging, diagnostics, therapy, and surgery. Challenging precision, safety, and selectivity requirements for ocular therapeutic and surgical procedures keep advancing the laser technologies, which in turn continue enabling novel applications for the preservation and restoration of sight. Modern lasers can provide single-cell-layer selectivity in therapy, submicrometer precision in three-dimensional image-guided surgery, and nondamaging retinal therapy under optoacoustic temperature control. This article reviews the evolution of laser technologies; progress in understanding of the laser–tissue interactions; and concepts, misconceptions, and accidental discoveries that led to modern therapeutic and surgical applications of lasers in ophthalmology. It begins with a brief historical overview, followed by a description of the laser–tissue interactions and corresponding ophthalmic applications.

## EARLY HISTORY

The concept of ocular phototherapy was first publicized by Dr. Gerhard Meyer-Schwickerath, who took patients to the roof of his laboratory in 1949 and focused sunlight on their retinas to treat melanomas (Meyer-Schwickerath 1960). Because the technique was hardly practical, nonsolar sources were sought. Xenon arc photocoagulator, which became available by the mid-1950s, was effective for sealing retinal breaks and treating tumors but was hard to use, and the burns were large and severe.

The development of laser in 1960 (Maiman 1960) revolutionized precision and control of light delivery because of several key distinctions from the noncoherent sources: (a) Photons are emitted at the same phase (and therefore are coherent); (b) wavelength range is very narrow (making it monochromatic light); and (c) the beam is very directional (it is well collimated) and hence can be tightly focused. Recognition of laser's potential for ocular therapy was almost immediate—the first report on making ocular lesions with a ruby laser was published the next year, in 1961 (Zaret et al. 1961). Although the results of ruby laser (694-nm wavelength) application were impressive, they were also troubling. The retinal burns were intense, and because the deep-red wavelength (694 nm) was poorly absorbed by melanin and blood, vascular closure could not be produced without either hemorrhage or intense scarring. The experience with iris photocoagulation was similar.

The discovery of the argon laser in 1964 (Bridges 1964) provided blue (488-nm) and green (514-nm) wavelengths, which had the advantage of being strongly absorbed by hemoglobin and melanin. Studies on the retinal application of the argon laser were soon underway (L'Esperance 1968), with several delivery systems including biomicroscopy (L'Esperance 1969). Further progress was achieved when the laser was coupled to a slit lamp (Little et al. 1970), providing an aiming beam and precise control of the spot size, location, power, and exposure duration. This delivery system enabled effective photocoagulation in a wider spectrum of retinal diseases, including small vascular lesions and a variety of maculopathies. The option of treating the trabecular meshwork (TM) and the iris was an obvious extension, and argon laser trabeculoplasty (ALT) (Teichmann et al. 1976, Wise & Witter 1979) and iridectomy (Beckman & Sugar 1973) were introduced in the 1970s. A series of clinical papers in 1971 signaled both the dissemination and acceptance of the new technology (Gass 1971, Patz et al. 1971, Pomerantzeff et al. 1971), which, in various iterations, remained the basis for clinical photocoagulation for the next 40 years.

Continuous progress in understanding of the laser–tissue interactions and advancements in laser technologies, together with discoveries of various tissue response pathways, keep advancing the precision and selectivity of the ocular laser therapy and surgery, and enable development of novel treatment strategies, which are reviewed below.

## PHOTOTHERMAL THERAPY

### Photothermal Interactions

Absorption of light in tissue leads to heating, and temperature is the governing parameter in all thermal laser–tissue interactions. Tissue effects depend on temperature and exposure duration and may include sublethal response to hyperthermia, as well as necrosis, coagulation, vaporization, and carbonization.

In addition to the laser irradiance  $I$  and absorption coefficient  $\mu_a$ , which depends on the laser wavelength, heat generation in tissue is determined by exposure time. If heat diffusion is neglected, then at a constant beam intensity the temperature rise is linear with time, shown by  $T(z, t) = \frac{\mu_a I(z)t}{\rho c}$ , where  $z$  is a three-dimensional space coordinate,  $\rho$  is tissue density and  $c$  is its heat capacity ( $c = 4.2 \text{ J/g/K}$ ,  $\rho = 1 \text{ g/cm}^3$  for water). Heat diffusion significantly reduces the temperature rise

if pulse duration exceeds the characteristic time necessary for heat to spread beyond the zone of light penetration in tissue. For the laser penetration depth  $L$ , the heat diffusion time is  $\tau = L^2/4\alpha$ , where  $\alpha$  is thermal diffusivity ( $\alpha = 1.4 \cdot 10^{-3} \text{ cm}^2/\text{s}$  for water). For example, for  $L = 1 \text{ }\mu\text{m}$  in water, the characteristic heat diffusion time is  $\tau = 1.7 \text{ }\mu\text{s}$ , whereas for  $L = 1 \text{ mm}$ , the diffusion time  $\tau = 1.7 \text{ s}$ . If pulse duration is comparable to or exceeds the characteristic diffusion time across the light absorption zone, then proper estimation of the peak temperature in tissue should take heat diffusion into account.

---

**RPE:** retinal pigmented epithelium

---

## Quantification of Thermal Damage

Temperature rise induces abnormal conformational changes in proteins and other biomolecules, which denature at characteristic rates specific to molecular species. Depending on the temperature and duration of the hyperthermia, these thermal processes may eventually lead to cell necrosis. Thermal damage to cells in a millisecond range of pulse durations can be approximated using the Arrhenius model (Niemz 2002, Sramek et al. 2009) of thermal denaturation. It assumes a rate of decline in the concentration of a critical molecular component  $D(t)$  with temperature  $T(t)$ :

$$dD(t) = -D(t) \cdot A \cdot \exp\left(-\frac{E^*}{R \cdot T(t)}\right) dt, \quad (1)$$

where  $E^*$  and  $A$  are the activation energy and rate constant parameterizing the process, and  $R = 8.3 \text{ J}/(\text{K} \cdot \text{mol})$  is the gas constant. Tissue damage, expressed as a decrease in critical molecular component  $D(\tau)$ , relative to its initial value  $D_0$  over the pulse length  $\tau$ , is represented by the Arrhenius integral  $\Omega$  as follows:

$$\Omega(\tau) = -\ln\left(\frac{D(\tau)}{D_0}\right) = A \int_0^\tau \exp\left(-\frac{E^*}{R \cdot T(t)}\right) dt. \quad (2)$$

The model assumes that irreversible tissue damage occurs when concentration of the critical molecular component drops below some threshold value. For example, if this threshold corresponds to a reduction in concentration by a factor of  $e$ , then  $\Omega = 1$ , and the remaining fraction of intact proteins is  $1/e \approx 37\%$ —or in other words, 63% of proteins have been damaged.

Measurements of the retinal pigmented epithelium (RPE) damage at various irradiation conditions yield the following average values (Sramek et al. 2009):  $E^* = 340 \text{ kJ/mol}$  and  $A = 1.6 \times 10^{55} \text{ s}^{-1}$ . It is important to keep in mind though that accurate estimation of cell survival under thermal stress is much more complex than just assessment of the denaturation rate of one type of protein or another. For example, (a) multiple types of proteins denature at different rates, (b) protein significance for cellular survival varies, and (c) cellular repair mechanisms cannot be ignored at long exposures. Therefore, the single values of the reaction rate  $A$  and activation energy  $E^*$  most likely represent characteristics of the so-called weak link in cellular metabolism—the most susceptible molecule to thermal damage—and may vary in different cell types.

The Arrhenius model fails to predict correct threshold temperatures at exposures longer than approximately 1 s because cellular repair mechanisms start playing a role at long exposures (Sramek et al. 2009). At pulse durations shorter than 50  $\mu\text{s}$  and temperatures below the vaporization threshold ( $\sim 100^\circ\text{C}$ ), the coagulation is insufficient for lethal damage, and therefore the dominant mechanism of damage at shorter pulses becomes mechanical—RPE cell rupture by vapor bubbles forming around overheated melanosomes (Schuele et al. 2005).

## Photocoagulation

Retinal photocoagulation typically involves application of laser pulses with durations ranging from 10 to 200 ms and transient temperature rise by tens of degrees. Laser energy is absorbed primarily

by melanin in the RPE and choroid and by hemoglobin in blood. Currently, the most common lasers in photocoagulation are frequency-doubled Nd:YAG (532 nm) and yellow semiconductor lasers (577 nm). Yellow wavelength has a slightly lower absorption coefficient in melanin than green has, but lower scattering of longer wavelength makes it less dependent on scattering in edematous retina or on other ocular opacities, which improves consistency and reproducibility of the photocoagulation (Sramek et al. 2012). At a 532-nm wavelength, only 5% of the incident laser energy is absorbed in the neural retina, approximately 45% in the RPE, and the rest in the choroid (Sramek et al. 2009). The generated heat diffuses from the RPE and choroid into the retina and causes coagulation of the photoreceptors and, sometimes, of the inner retina. During 100-ms application the heat diffuses by up to 200  $\mu\text{m}$ , thus “smoothing” the edge and extending the coagulated zone beyond the boundaries of the laser spot; this effect is termed thermal blooming. When one uses shorter pulses and smaller spot sizes, heat diffusion can be limited to the photoreceptor layer (approximately 70  $\mu\text{m}$  in thickness), thereby avoiding the inner retinal damage.

Photocoagulation was proven safe and effective in treatment of proliferative diabetic retinopathy. In this disorder, the retina becomes ischemic and releases a variety of chemical messengers, most importantly vascular endothelial growth factor (VEGF), and these cytokines stimulate the growth of new blood vessels and increase retinal vascular permeability. The abnormal new vessels, associated fibrous tissue, and macular edema are major causes of the sight-threatening complications in diabetic eye disease. The premise for initial introduction of lasers to treatment of proliferative diabetic retinopathy in 1969 (Beetham et al. 1970) was based on observation that patients with retinal scars (which lack photoreceptors) do not develop neovascularization. Beetham, Aiello, and coauthors (1970) then suggested that creating retinal scars by laser photocoagulation may help prevent the proliferative phase of diabetic retinopathy. This premise now appears erroneous, and elimination of just a significant fraction (approximately 30%) of photoreceptors (the metabolically most active and most numerous cells in the retina) reduces metabolic demand and thereby decreases production of angiogenic factors. Scarring appears to be a secondary phenomenon associated with the loss of photoreceptors but is not a requirement. In fact, it can be minimized in photocoagulation, as discussed below.

Coagulation of a large fraction of photoreceptors (approximately 30%) in the peripheral retina (**Figure 1**) has been termed panretinal photocoagulation (PRP), and it significantly reduces the risk of central vision loss due to neovascularization (Diabet. Retinopathy Study Res. Group 1981, Early Treat. Diabet. Retinopathy Study Res. Group 1991). The side effects of PRP—mild nyctalopia (difficulty seeing at low light) and reduction of the peripheral visual field—are outweighed by preservation of the central vision (Diabet. Retinopathy Study Res. Group 1981).

**Retinal plasticity following photocoagulation.** Initially, relatively long pulses (100–200 ms) have been used to produce rather intense lesions in retinal coagulation (Diabet. Retinopathy Study Res. Group 1981). Effects of an intense retinal burn produced by a 100-ms laser pulse include acute full thickness injury shown in **Figure 2a**, resulting in permanent scarring shown in **Figure 2b**. Such intense lesions are unacceptable because they destroy not only photoreceptors but also the nerve fiber layer, thereby creating large arc defects in the visual field. More conventional lesions at present are so-called light burns, illustrated in **Figure 2c–d**. Photoreceptors are damaged, but the inner nuclear layer and ganglion cells are very well preserved, although light burns also result in permanent scarring, as shown in **Figure 2d**. In intense burns, these scars tend to expand over time, thereby enlarging the scotomata (Maeshima et al. 2004, Schatz et al. 1991).

Interestingly, in small and very light lesions (minimally visible or barely visible clinical grades), the glial scar forming in place of the destroyed photoreceptors contracts over time, and photoreceptors shift from adjacent areas into the lesion, as shown in **Figure 3**. In this process, the



**Figure 1**

Fundus of a patient with diabetic retinopathy after panretinal photocoagulation. All the peripheral retina beyond the vascular arcades is treated with lesions (*light round spots*) coagulating photoreceptors and retinal pigmented epithelium, but preserving the inner retina. Elimination of up to 30% of the photoreceptors, the metabolically most active and numerous cells in the retina, reduces oxygen consumption and thereby decreases angiogenic signaling, preventing neovascularization and sparing the central vision.

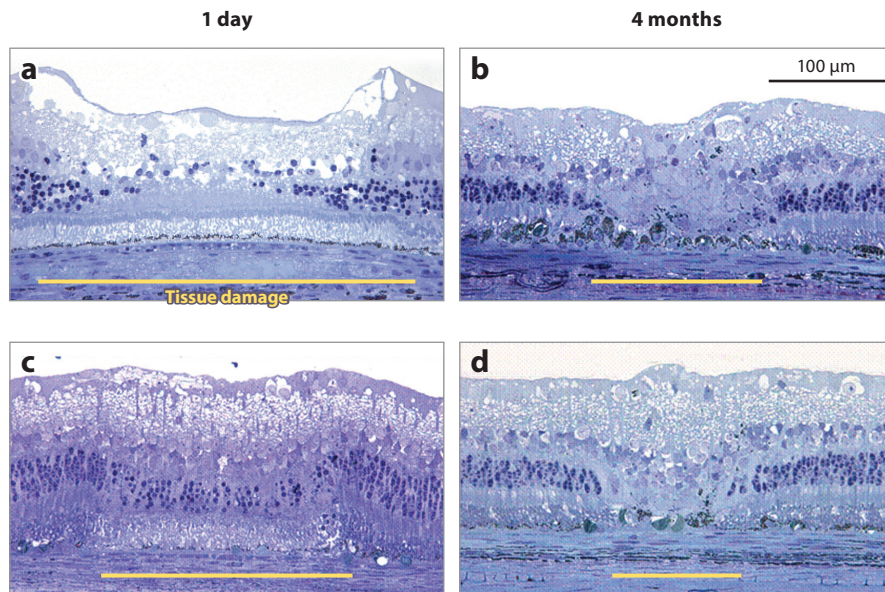


**Figure 2**

An intense burn in a rabbit retina produced by 100-ms laser pulses, including full thickness injury and early necrotic features (*a*) 1 day after treatment and (*b*) 4 months after treatment. (*c*) Light burn exhibits damaged photoreceptors at 1 day, but the inner nuclear layer and ganglion cells are preserved. (*d*) Residual permanent scarring of the light burn at 4 months. Large scars tend to slowly expand over time (so-called scar creep), further extending the scotoma. Figure adapted from Paulus et al. (2008).

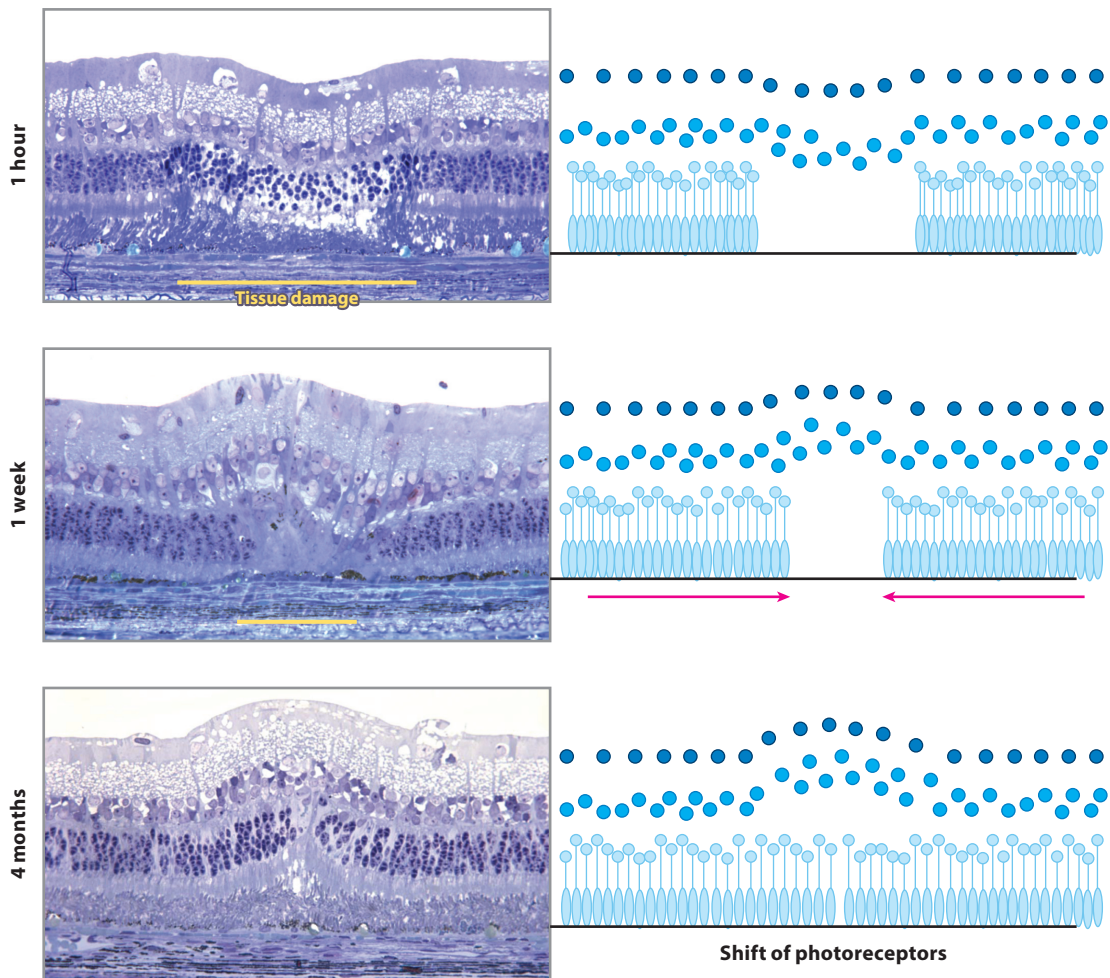


**Figure 3**

Migration of the photoreceptors into the very light lesion of 200  $\mu\text{m}$  in width restores continuity of the photoreceptor layer over time and prevents formation of a scotoma and scarring. Shifted rods and cones rewire to the local rod- and cone-bipolar cells, restoring retinal neural network in the lesion, including proper function of the on and off pathways. Figure adapted from Sher et al. (2013).

migrating photoreceptors rewire to the local deafferented bipolar cells, restoring on and off retinal signal pathways in the lesion (Sher et al. 2013). This process allows achievement of the goal of PRP—reduction of the retinal metabolic load by destroying a significant fraction of photoreceptors (approximately 30%), metabolically the most active and the most numerous cells in the retina, while avoiding the deleterious side effects of scotomata and scarring, which degrade peripheral vision. A similar phenomenon of restorative retinal plasticity has been recently observed in rats (Belokopytov et al. 2010) and in primates (Merigan et al. 2011).

**Optimization of pulse duration.** Owing to heat diffusion, lesion diameter increases with pulse duration. Therefore, the more confined and better-healing lesions can be achieved using shorter pulses. Another benefit of shorter exposures is the reduced sensation of pain (Muqit et al. 2010,

Nagpal et al. 2010) owing to decreased diffusion of heat into the choroid, where pain receptors are located.

Because the Arrhenius integral scales linearly with pulse duration (Equation 2), higher temperatures are required to achieve the same clinical grade with shorter pulses (Jain et al. 2008). In addition, higher power is required to deliver the same energy with shorter pulses. If temperature exceeds the vaporization threshold, transient vapor bubble may result in retinal rupture. As illustrated in **Figure 4a**, for pulse durations of 20, 50, and 100 ms, all the grades (light, moderate, intense, very intense) could be created with appropriate choice of power settings, without retinal rupture. At pulse durations below 10 ms, creating intense lesions without inadvertently rupturing the retina becomes increasingly difficult. At 1 ms, there was practically no difference between the power required to create a mild retinal lesion and that required to produce a rupture.

The ratio of the threshold power producing a rupture to that required for producing a light lesion is defined as the therapeutic window and represents one means of quantifying the safe dynamic range of retinal photocoagulation. The larger this ratio, the greater is the margin of

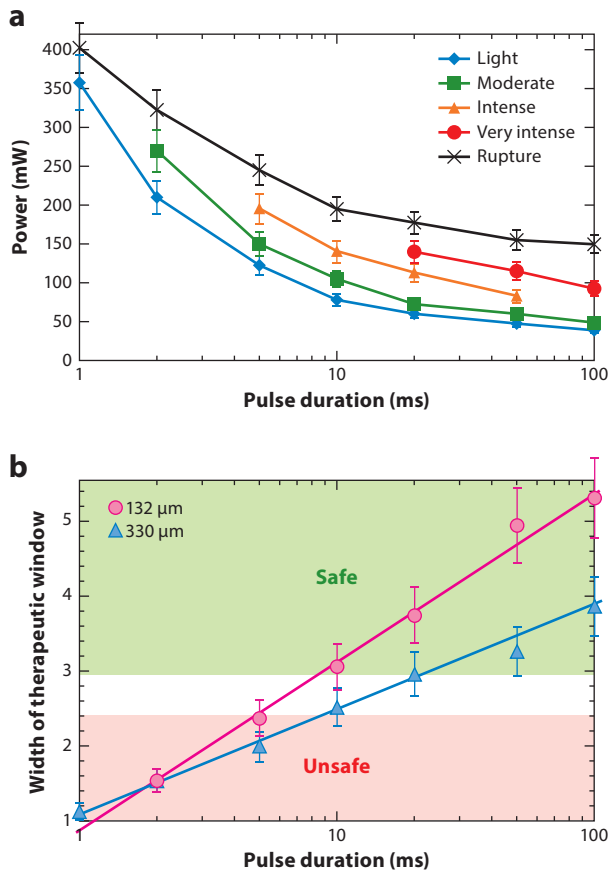


**Figure 4**

(a) Laser power required to create retinal lesions increases with decreasing pulse duration (measured with 132- $\mu\text{m}$  spot size on the retina). (b) The range of powers between photocoagulation and rupture (the therapeutic window) decreases with decreasing pulse duration, making visible photocoagulation unsafe with pulses shorter than 10 ms.

safety to create a visible lesion without inadvertently inducing a retinal rupture. **Figure 4b** depicts the width of this therapeutic window as a function of pulse duration for two different laser spot sizes. As pulse duration decreases from 100 to 1 ms, the width of the therapeutic window declines from 3.9 or 5.4 to 1, for 132- $\mu\text{m}$  or 330- $\mu\text{m}$  retinal spot sizes, respectively. The width of the safe therapeutic window should suffice to accommodate for variations in fundus pigmentation, which typically do not exceed a factor of 2. To provide a safe therapeutic window larger than 2.5, pulse durations should exceed 10 ms for a 330- $\mu\text{m}$  beam diameter, and 20 ms for the 132- $\mu\text{m}$  spot size.

It is important to keep in mind that coagulation of blood vessels requires more energy than other tissue does owing to cooling by the blood flow. For example, if a spot size of 100  $\mu\text{m}$  with exposure time of 100 ms is applied to occlude a blood vessel with flow velocity of 5 mm/s, the laser energy is effectively distributed over the 0.5-mm length of the blood vessel, which is five times larger than the width of the laser spot. Thus, the temperature at the photocoagulation site is significantly lower than it would be in stationary tissue.

**Laser trabeculoplasty.** With the advent of the slit-lamp-based laser delivery system, the option of treating the iris and TM was an obvious application, and argon laser was first introduced for iridectomy (Beckman & Sugar 1973) and trabeculoplasty (Teichmann et al. 1976, Wise & Witter 1979) in the 1970s. Both procedures were designed to create holes in the iris and in TM to improve aqueous outflow and reduce intraocular pressure (IOP) in cases of closed- and open-angle glaucoma, respectively. Safety and efficacy of the ALT (see **Figure 5**) in subjects with newly diagnosed primary open-angle glaucoma were demonstrated in 1995 (Glaucoma Laser Trial Res. Group 1995). With argon laser (514 nm) or more recently with the equivalent 532-nm Nd:YAG laser, 50 spots of 50  $\mu\text{m}$  in diameter are applied to the 180° on TM with pulses of 100 ms in duration. Intraocular pressure decreases by 25%–30%, and the effect lasts for several years, although it diminishes over time. Because laser burns in TM are much larger than the beam size and they scar over time, retreatment of the same areas is not possible.

**Real-time monitoring of tissue temperature.** Owing to the strong variation in fundus pigmentation and transparency of the ocular tissues from patient to patient, and even between different areas in the same eye, the same laser settings may lead to very different results. Therefore, direct measurement of retinal temperature during photocoagulation would help for providing uniform outcomes, especially when the treatment is subvisible.

A noninvasive method of measuring RPE temperature has been developed, based on detection of acoustic waves generated in melanosomes irradiated with nanosecond laser pulses (Schuele et al. 2004). An acoustic transducer built into a contact lens, which is attached to the treated eye during the procedure, detects the pressure waves generated due to thermal expansion of melanosomes upon absorption of nanosecond laser pulses. The thermoelastic expansion coefficient of water varies with temperature by approximately 1% per 1°C (Schuele et al. 2004), and this effect allows for monitoring the changes in temperature of the RPE cells by detecting the changes in amplitude of acoustic waves generated by the laser pulses of constant energy. The probing laser pulses are applied simultaneously with application of a therapeutic laser to detect temperature rise in tissue during the exposure. Precision of this method is on the order of 1°C, and this feedback is then used to adjust laser power or pulse duration to ensure predictable outcome of photocoagulation (Koinzer et al. 2015).

**Pattern-scanning laser photocoagulation.** As described above, smaller and lighter lesions heal with less scarring, or even no scarring at all. However, for clinical efficacy of photocoagulation with smaller and lighter lesions to be maintained, a larger number of spots should be applied to

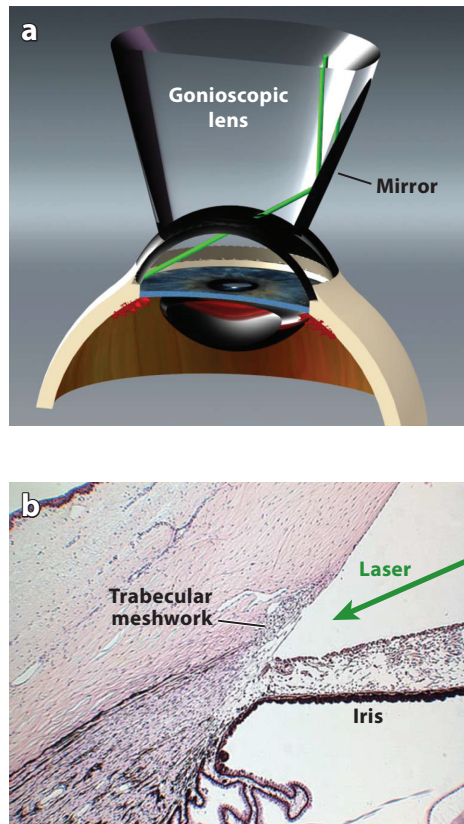


**Figure 5**

(a) Laser is guided onto the trabecular meshwork (TM) via gonioscopic lens for treatment of the open-angle glaucoma. (b) Histology of the anterior angle of the human eye with illustration of the incoming laser beam directed onto the TM.

provide the same total coagulated area (Palanker et al. 2011). Manual application of hundreds or even thousands of spots is fatiguing for both physician and patient, and maintaining constant spot density is rather difficult. The first attempts to automate photocoagulation involved rather complex equipment, including image recognition software and eye tracking (Wright et al. 2000). Complexity of such systems prevented their commercial introduction and acceptance in clinical practice.

A semiautomatic pattern-scanning photocoagulator (PASCAL, Topcon Medical Laser Systems Inc.) was introduced by OptiMedica Corp. in 2005 (Blumenkranz et al. 2006). It delivers patterns of laser spots in a rapid succession, activated by a single depression of a foot pedal. Patterns include square arrays with up to  $5 \times 5$  spots, arcs with adjustable numbers of concentric rows, circular patterns for photocoagulation of small retinal holes, and rings and arcs with adjustable central exclusion zones for application around the fovea. To deliver the whole pattern within the eye fixation time, each exposure should be shorter than in conventional photocoagulation: 10–20 ms instead of 100–200 ms, traditionally applied with single spots.

Because lighter lesions produced with shorter pulses are smaller than more intense burns produced with longer exposures, applying more of them and at higher density is important to

**CNV:** choroidal neovascularization

**AMD:** age-related macular degeneration

**DME:** diabetic macular edema

**CSCR:** central serous chorioretinopathy

**TTT:** transpupillary thermotherapy

ensure the same total area is coagulated in PRP. For example, instead of 1,000 moderate-grade lesions produced with 400- $\mu\text{m}$  laser spots using 100-ms pulses, one needs to apply 1,461 lesions of the same grade with 20-ms pulses, 1,971 light-grade lesions with 20-ms pulses, or 3,528 barely visible lesions with 20-ms exposures (Palanker et al. 2011).

Even more automated laser delivery, guided by diagnostic imaging and stabilized using eye tracking, has been introduced in a Navilas system (OD-OS GmbH). This system includes retinal image acquisition, annotation of the images to create a detailed treatment plan, and then automated laser delivery to the retina according to the treatment plan. This system is particularly useful for image-guided targeting of the leaking microaneurysms (Kozak et al. 2011).

## Nondamaging Laser Therapy of the Macula

In the past, laser photocoagulation was used to treat extrafoveal choroidal neovascularization (CNV), which occurs in wet age-related macular degeneration (AMD). Intense photocoagulation destroys the invading vasculature but usually leaves a chorioretinal scar and associated blind spot (scotoma). Even though the treatment outside the center of the macula is typically well tolerated by the patients, currently, a vast majority of physicians use anti-VEGF pharmacotherapy because it avoids scarring in the macula. Similarly, anti-VEGF injections are replacing the laser coagulation of the leaking microvascular abnormalities in branch retinal vein occlusion (BRVO) and in proliferative diabetic retinopathy.

Grid photocoagulation for treatment of the diabetic macular edema (DME) and central serous chorioretinopathy (CSCR) was shown to be efficient (Writ. Comm. Diabet. Retinopathy Clinic. Res. Netw. 2007), but its mechanism of action was never understood. There is a growing body of clinical evidence that many macular diseases, such as CSCR, DME, and BRVO, can be successfully treated without tissue damage.

The nondamaging approach to retinal laser therapy was initially attempted using near-infrared diode laser (810 nm) with very long exposures (60 s) and a millimeter-wide spot on the retina (Reichel et al. 1999). This approach, termed transpupillary thermotherapy (TTT) (Newsom et al. 2001), has been tested in treatment of CNV in AMD (Newsom et al. 2001, Reichel et al. 1999). Proponents of this approach have hypothesized that there is a selective damaging effect of heating on actively dividing cells in newly formed blood vessels owing to their higher susceptibility to thermal injury than nondividing cells have in normal tissue. The estimated retinal temperature elevation with TTT at clinical settings (810 nm, 800 mW, 60 s, 3-mm spot size) is approximately 10°C (Mainster & Reichel 2000). The mechanism of treatment of CNV by TTT may occur through vascular thrombosis, apoptosis, or the thermal inhibition of angiogenesis (Mainster & Reichel 2000). The users of TTT encountered difficulties with reliable titration, resulting in frequent occurrences of significant retinal damage (Benner et al. 2002).

Later, a pulsed version of a similar laser with smaller spot size (125  $\mu\text{m}$ ) was applied to nondamaging retinal therapy. The so-called micropulse laser delivers 100–300-ms long bursts composed of 0.1- to 0.3-ms pulses, repeated at a 500-Hz rate. The average power during the burst is set below the clinically detectable tissue damage by adjusting the peak power and pulse duty cycle (pulse duration divided by pulse period) in the range of 5% to 15% (Dorin 2004).

Clinical trials have shown that micropulse treatment of DME delivered with high-spot density is equally efficient as or superior to the standard mETDRS protocol (Lavinsky et al. 2011). Other clinical trials demonstrated that the micropulse-laser treatment reduced the subretinal fluid and improved visual acuity in patients with CSCR, compared to untreated control groups (Roisman et al. 2013). The procedure also exhibited equivalent clinical efficacy to conventional lasers in treatment of macular edema secondary to BRVO but without the tissue damage

(Parodi et al. 2006). However, the lack of a well-defined titration procedure is reflected in variable results of these studies (Figueira et al. 2009, Sivaprasad et al. 2010, Venkatesh et al. 2011). In addition, high-density coverage of the macula with small spots and long pulses requires a lengthy treatment.

Significant advantages of the nondamaging retinal phototherapy are the absence of scotomata and scarring, the ability to treat foveal areas, and improved preservation of color vision and contrast sensitivity (Sivaprasad et al. 2010). The lack of chorioretinal damage permits high-density coverage, which greatly improves therapeutic outcomes compared to conventional sparse laser treatment protocols in the macula (Lavinsky et al. 2011). Nearly confluent laser applications could be safely delivered over the entire edematous areas if short pulse treatment and pattern scanning are applied. This approach allows retreatment of the same areas, even in the fovea.

Dynamic range of the retinal response to nondamaging hyperthermia has been established by monitoring expression of the heat shock protein HSP-70 in mice (Sramek et al. 2011). On the basis of these results, a titration protocol for adjustment of the laser power and duration was developed (Lavinsky et al. 2014). This protocol, called Endpoint Management (EpM), ties the subvisible tissue effects to a visible titration. Laser power is first titrated to produce a barely visible lesion at 15- or 20-ms pulse duration, and this energy is set to be 100% on the EpM scale. Experiments with heat shock protein (HSP) expression following nondamaging retinal exposures in mice (Sramek et al. 2011), as well as a computational analysis of the clinical laser settings (Luttrull et al. 2012), indicated that nondestructive thermal therapy corresponds to Arrhenius values within the range of approximately  $0.1 < \Omega < 1$  (Figure 6). In this regime, the RPE cells survive the hyperthermia and respond to thermal stress by expression of HSPs. At higher settings ( $\Omega > 1$ ), the RPE gets damaged, but below  $\Omega \sim 10^2$ , the lesions are ophthalmoscopically invisible, at least not immediately after the laser application. Immediately visible lesions produced at higher laser settings result in lethal damage to RPE and photoreceptors and have calculated values of  $\Omega > 10^3$

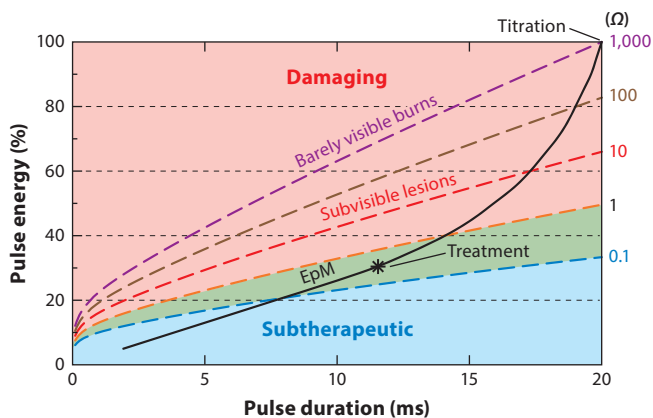


**Figure 6**

Endpoint Management protocol (EpM). Dashed lines correspond to lesions of various clinical grades, with the Arrhenius integral  $\Omega = 10^3$  corresponding to barely visible lesions,  $\Omega = 1$  corresponding to retinal pigmented epithelium damage threshold, and  $\Omega = 0.1$  corresponding to the lower end of the heat shock protein expression range. When the laser power and pulse duration are adjusted, EpM (solid line) relates 10× steps in  $\Omega$  to 20% steps in pulse energy. Damaging range ( $\Omega > 1$ ) is shown in red, nondamaging treatment range ( $0.1 < \Omega < 1$ ) is shown in green, and subtherapeutic range ( $\Omega < 0.1$ ) is shown in blue. The 30% energy on the EpM scale in the middle of the nondamaging treatment range is shown by an asterisk. Figure adapted from Lavinsky et al. (2016).

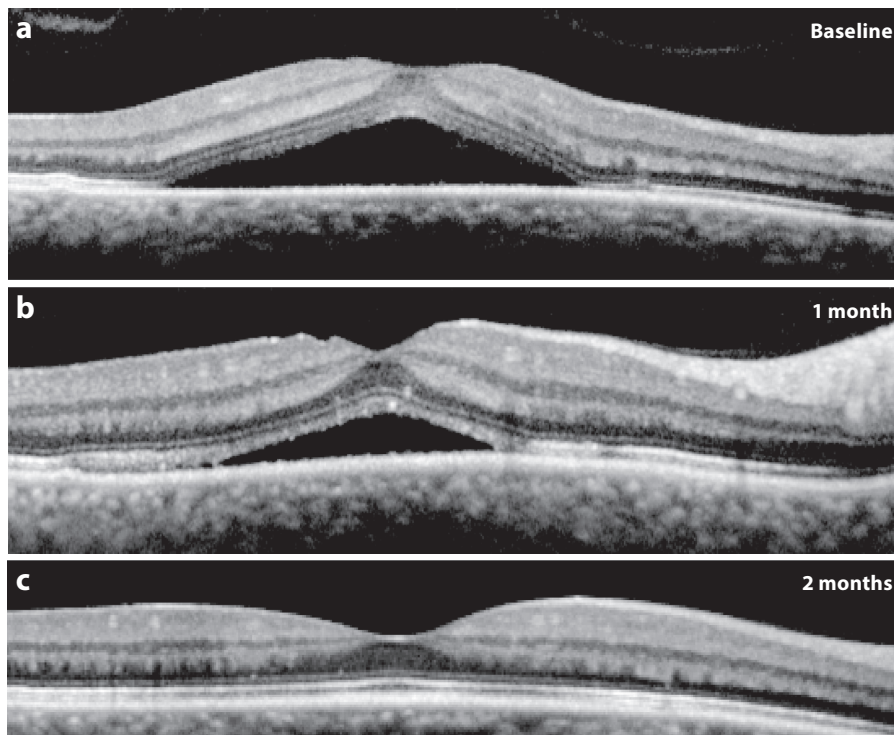


**Figure 7**

Resolution of subretinal fluid in a patient with chronic central serous chorioretinopathy after nondamaging retinal laser therapy. Approximately 400 spots have been applied at 30% Endpoint Management energy, and no tissue damage has been detected during the 12-month follow-up. (a) Visual acuity at baseline was 20/100, and it improved to (b) 20/40 at 1 month and (c) 20/20 at two months. Figure adapted from Lavinsky & Palanker (2015).

(**Figure 6**). By adjusting the pulse duration and power, the EpM algorithm maps logarithmic steps ( $10\times$ ) of Arrhenius integral values to linear steps (20%) in pulse energy, normalized to a titration dose (Lavinsky et al. 2014), as shown in **Figure 6**.

With 200- $\mu\text{m}$  spot size, the threshold of RPE damage was found to be 30% on the EpM scale (Lavinsky et al. 2014). Operating below the damage threshold allows the application of high-density patterns to increase clinical efficacy. Spot spacing of 0.25–spot diameter (50  $\mu\text{m}$ ) is typically applied. A treatment zone with a radius of 3 mm includes approximately 400 spots. This nondamaging protocol has been recently tested in treatment of chronic CSCR using 30% energy settings (Lavinsky & Palanker 2015). The trial demonstrated lack of tissue damage and excellent response to the treatment (**Figure 7**) and to retreatments (Lavinsky et al. 2016). Additional clinical trials of this methodology in applications to DME, CSCR, macular telangiectasia, and dry AMD are in progress.

**NRT:** nondamaging retinal laser therapy

**Patterned laser trabeculoplasty.** Patterned laser trabeculoplasty (PLT) has recently been introduced for subvisible or nondamaging treatment (Turati et al. 2010). Its computer-guided patterns provide dense coverage of TM with 5-ms-long subvisible exposures—a strategy similar to the nondamaging retinal laser therapy (NRT) described above. As with NRT, laser power is first

titrated to a barely visible burn in the area of highest pigmentation (the inferior segment) using 10-ms pulses, and then pulse duration is decreased by half to reduce the energy below the visible damage threshold. Reduction in IOP following this treatment (~25%) was similar to the results of ALT (Barbu et al. 2014, Turati et al. 2010) and, owing to lack of tissue scarring, it allows periodic retreatments.

---

**PDT:** photodynamic therapy

---

## **SELECTIVE TARGETING OF TISSUE WITH PHOTOCHEMICAL INTERACTIONS: PHOTODYNAMIC THERAPY**

Photochemical interactions are based on nonthermal light-induced chemical reactions. To avoid heating, photodynamic therapy (PDT) is performed at very low power densities (typically  $<1 \text{ W/cm}^2$ ) and using minute-long exposures. For PDT, special chromophores, called photosensitizers, are injected intravenously and allowed to accumulate in the target tissues. Upon excitation by laser radiation, the photosensitizer produces highly cytotoxic reactants—free radicals or singlet oxygen, which, in turn, produce irreversible oxidation of the nearby cell structures.

The concept of treating exudative AMD by selectively targeting vascular endothelial cells using a specific photosensitizer-carrier complex activated by near-infrared laser was adapted from tumor therapy (Dougherty & Mang 1987, Schmidt et al. 1992). Following successful initial results with phthalocyanine, liposomal benzoporphyrin derivative (verteporfin or Visudyne) was developed, which selectively attaches to endothelium of new blood vessels (Kramer et al. 1996, Miller et al. 1995). This differential accumulation is the basis for selectivity of PDT against neovascularization, compared with the normal choroidal and retinal vasculature.

The far-red peak (688–691 nm) of the verteporfin absorption spectrum is typically utilized in clinical practice because of the lower retinal sensitivity and its superior penetration into the choroid (Woodburn et al. 2002). Closure of the abnormal blood vessels occurs within approximately 6–12 weeks in most patients (Schmidt-Erfurth et al. 1994, Verteporfin Photodyn. Ther. Study Group 2001). Reperfusion is common, and multiple treatments are often required.

Since the recent advent of anti-VEGF pharmacotherapy, which has proven to be much more efficient in the prevention of neovascularization, PDT has fallen out of favor, and its infrequent use in the United States is now limited to chronic CSCR (Oh & Yu 2015).

## **PHOTOMECHANICAL INTERACTIONS**

Vapor bubbles produced when tissue temperature exceeds the vaporization threshold may rupture cells within a zone comparable to the bubble size. The actual temperature required for vaporization varies between 100°C and 305°C, depending on pulse duration and on the presence of the bubble nucleation sites (Vogel & Venugopalan 2003). For efficient heating, the energy should be delivered fast enough to avoid heat diffusion during the pulse, a condition called thermal confinement. In other words, laser pulse  $\tau$  should be shorter than the time required for heat diffusion from the zone of laser absorption:  $\tau < L^2/4\alpha$ , where  $L$  is the light penetration depth in tissue ( $L = 1/\mu_a$ ) and  $\alpha$  is the thermal diffusivity of tissue. For example, with  $L = 1 \text{ }\mu\text{m}$ ,  $\tau$  should not exceed 1.7  $\mu\text{s}$ . Precise tissue ablation requires the use of laser wavelengths corresponding to a small optical penetration depth in tissue in order to confine the energy deposition to a small volume.

Much shorter pulses may produce stress confinement—a condition in which an acoustic wave generated by thermal expansion of the material cannot escape from the heated zone during the laser pulse. Because the velocity of sound in water is approximately  $v = 1.5 \text{ km/s}$ , the stress confinement conditions are achieved within the  $L = 1 \text{ }\mu\text{m}$  penetration depth if pulse duration does not exceed  $\tau = L/v = 0.7 \text{ ns}$ . Such conditions may promote the generation of powerful stress waves, which

**SRT:** selective retinal pigmented epithelium (RPE) therapy

**SLT:** selective laser trabeculoplasty

propagate with supersonic velocities and may result in tissue disruption (Vogel & Venugopalan 2003).

Vaporization of water in an overheated volume results in the formation of a short-living (on the order of microseconds) vapor bubble that expands, cools, and collapses (cavitation) during the time determined by its maximum radius (Young 1989). These bubbles are not visible to the eye during surgery, but they can be easily visualized using fast flash photography.

Explosive vaporization produced by microsecond pulses of Er:YAG laser ( $\lambda = 2.94 \mu\text{m}$ ,  $L \approx 1 \mu\text{m}$  in water) has been applied to the dissection of epiretinal membranes in front of the fiber probe (D'Amico et al. 1996a,b). Alternatively, overheating of liquid with nanosecond argon fluoride (ArF) excimer laser ( $\lambda = 193 \text{ nm}$ ) strongly absorbed in proteins ( $L \approx 0.2 \mu\text{m}$  in tissue) has been applied to the dissection of epiretinal and subretinal membranes (Hemo et al. 1997, Palanker et al. 1994). Despite the early promise of these devices in clinical tests, both have failed to achieve acceptance in practice owing to the cost, fiber rigidity, and lack of coagulation capability.

### Selective RPE Therapy

Light is strongly absorbed by melanosomes in the RPE ( $\mu_a \approx 8,000 \text{ cm}^{-1}$ ) (Brinkmann et al. 2000). Application of microsecond laser pulses allows for confinement of the thermal and mechanical effects of this absorption within the RPE layer, thus sparing the photoreceptors and the inner retina (Roeder et al. 1992, 1993). Microsecond and nanosecond pulses can selectively damage RPE by formation of small cavitation bubbles around melanosomes (Schuele et al. 2005). Microsecond exposures can also be conveniently produced by rapid scanning of a continuous laser beam. For example, scanning a beam of  $d = 100 \mu\text{m}$  in diameter with a speed of  $v = 10 \text{ m/s}$  produces exposures of  $t = d/v = 10 \mu\text{s}$  in duration on the epithelial cells, sufficiently short for selective treatment of the RPE (Framme et al. 2007, Paulus et al. 2010) (**Figure 8a,b**). Subsequent RPE proliferation and migration restores continuity of the RPE layer within a few days, resulting in normalization of the photoreceptor outer segments in the treated area (**Figure 8d-f**).

Several small clinical studies have demonstrated the efficacy of selective RPE therapy (SRT) in treatment of DME, CSCR (Elsner et al. 2006), and subfoveal fluid after rhegmatogenous retinal detachment (Brinkmann et al. 2006, Koinzer et al. 2008). Despite its clinical promise, this technique has not been commercialized yet. One of the difficulties with SRT is the lack of visible change in the retina, making the assessment of adequate laser dosimetry in every patient difficult. An acousto-optical system has been developed that may help assess the cavitation threshold energy in RPE (Brinkmann et al. 2001). Alternatively, light scattering by cavitation bubbles measured with a short flash could be used for this diagnostic.

### Selective Laser Trabeculoplasty

Selective laser trabeculoplasty (SLT) was introduced in 1995 (Latina & Park 1995, Latina et al. 1998) by Mark Latina in the Wellman Labs at approximately the same time that SRT was developed in an adjacent room. As in SRT, the short pulses of light absorbed in pigmented cells cause explosive vaporization of melanosomes, leading to destruction of the pigmented endothelial cells lining the meshwork beams, while sparing the nearby nonpigmented tissue. SLT systems include a Q-switched, 532-nm laser that delivers 3-ns pulses in a 400- $\mu\text{m}$  spot. In contrast to ALT, which results in scarring of the TM (Wise & Witter 1979), SLT leaves the meshwork intact (Latina et al. 1998). With a 400- $\mu\text{m}$  beam, 100 spots provide practically complete coverage of the TM. As in SRT, epithelial cells migrate and proliferate to repopulate the TM, and it is hypothesized that in this process, the deposits clogging the TM are removed, resulting in improved permeability to

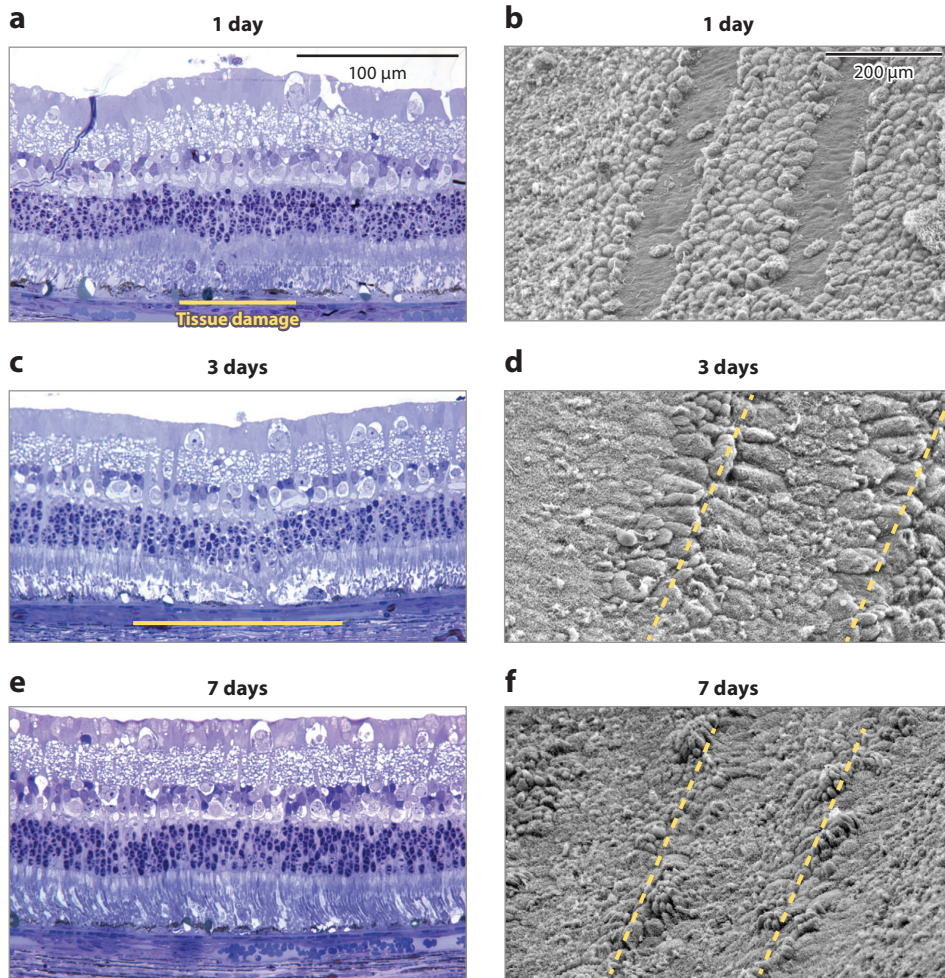


**Figure 8**

(a) Retinal pigmented epithelium (RPE) is selectively damaged by a rapidly scanning 532-nm laser. With a spot size of 100  $\mu\text{m}$  and scanning velocity of 6.6 m/s, the exposure time is 15  $\mu\text{s}$ . (b) Scanning electron microscopy (SEM) one day after the treatment reveals the laser scanning lines surrounded by the intact RPE. (c) Three days after treatment, RPE stretches into the lesion, but outer segments of photoreceptors are still abnormal. (d) SEM shows the damaged areas covered by the RPE migrated and stretched from the intact areas. (e) Seven days after treatment, RPE and outer segments are restored. (f) SEM shows complete, albeit uneven, coverage of RPE in the treated areas, including smaller, newly proliferated RPE cells.

aqueous outflow, leading to reduction of IOP. SLT has been shown effective in treatment of open-angle glaucoma (Latina et al. 1998, Melamed et al. 2003, Nagar et al. 2005), thereby proving that permeability of TM to aqueous flow can be improved without destruction of its microstructure. SLT is easier to perform owing to its larger spot size and is better tolerated by patients because of reduced pulse energy. Similar to that of ALT, the IOP-lowering effect of SLT lasts for several years, but it also diminishes over time. However, unlike in ALT, lack of scarring in SLT allows retreatment.

## REFRACTIVE SURGERY

The first ideas for reshaping the cornea to correct refractive errors were published by Lendeer Jans Lans from Holland in 1896, when he proposed using penetrating corneal cuts to correct astigmatism. In 1930, the Japanese ophthalmologist Tsutomu Sato demonstrated that radial cuts in the cornea could indeed correct up to six diopters. However, this procedure was not accepted in practice owing to the high rate of associated corneal degeneration. In 1974, Svyatoslav N. Fedorov (also spelled Fyodorov) in Moscow, Russia, began popularizing this procedure for correction of myopia. The first attempts at corneal carving—a technique termed keratomileusis—started in 1963 in the Ignacio Barraquer clinic in Bogotá, Colombia. But the initial surgical maneuvers were inherently imprecise, and modern refractive surgery dates to an accidental discovery in 1980.

Rangaswamy Srinivasan, a scientist in James Wynne's group at the Watson Research Center of IBM, was studying the application of a newly developed 193-nm ArF excimer laser to material processing. In October 1981, Srinivasan and Wynne put turkey cartilage left over from Thanksgiving dinner under the laser beam and observed a beautiful crater formed by ablation—much cleaner than any other laser they had tested (Srinivasan et al. 1983). The process exhibited a previously unattainable level of exactitude—down to  $0.2\ \mu\text{m}$ —and, owing to lack of thermal damage, was originally believed to be purely photochemical, whereby absorption of high-energy photons ( $E = 6.4\ \text{eV}$ ) led to decomposition of molecular bonds and material ejection because of the increased volume of the photofragments (Garrison & Srinivasan 1985, Srinivasan & Leigh 1982). The process was termed photoablation (initially, ablative photodecomposition) to reflect this new mechanism, and it is described as such in many textbooks today. However, further research revealed that the quantum yield of photochemical bond-breaking is insufficient to explain ablation thresholds and that vaporization of water in the cornea is actually responsible for material ejection (Kitai et al. 1991). Lack of detectable thermal damage was due to (a) very shallow penetration depth in tissue ( $0.2\ \mu\text{m}$  in the cornea) and (b) thermal confinement of the very short (10-ns) pulses (Isner & Clarke 1987, Telfair et al. 2000).

Stephen Trokel and Francis L'Esperance of Columbia University first thought to use this laser as a replacement for a scalpel in radial keratotomy; however, a revolutionary approach of direct ablation of the corneal surface (termed photorefractive keratectomy, or PRK) has proven to be the most promising, and the first procedure was performed in 1983 (Trokel et al. 1983). Later, problems of slow and rather uncomfortable recovery of the epithelial layer were eliminated by first cutting a flap in the cornea, which is pulled back to expose the corneal bed for laser ablation—a procedure widely used today in clinical practice and called laser-assisted in situ keratomileusis (LASIK) (Pallikaris et al. 1991).

Another revolutionary step in refractive surgery was the development of the femtosecond laser for corneal flap cutting, pioneered by Tibor Juhasz's group in 1998 (Kurtz et al. 1998). The mechanism of plasma-mediated interactions of ultrafast lasers with transparent tissue is described in the next section. Unlike mechanical microkeratome, laser cutting enabled formation of vertical walls around the planar flap, and this process provided better positioning of the corneal flap back into the original location after ablation. This improved the consistency of refractive outcomes and led to wide acceptance of the femtosecond laser in refractive surgery (Nordan et al. 2003, Ratkay-Traub et al. 2001). Later, ultrafast lasers would also enable refractive surgical procedures based on intrastromal cutting without the excimer laser ablation: extraction of lenticules (Heisterkamp et al. 2003) and producing pockets for intrastromal rings (Ertan & Bahadir 2006). The same laser systems have been applied to transplantation of the whole cornea and corneal endothelium (Jonas 2004), or so-called endothelial keratoplasty.

## TRANSPARENT TISSUE SURGERY WITH ULTRASHORT-PULSE LASERS

Transparent tissue can be dissected utilizing a nonlinear process of material ionization by a high intensity laser beam. At extremely high irradiances ( $10^8$ – $10^{11}$  W/cm<sup>2</sup>), which can be achieved in a short-pulsed (nanosecond to femtosecond) tightly focused laser beam, transparent material can be ionized, and ions absorbing the laser light reach very high temperatures (Vogel & Venugopalan 2003). This mechanism, called dielectric breakdown, allows for highly localized energy deposition at the focal point of the laser beam, even inside a transparent medium. This process is widely used in fragmentation of the opacified posterior lens capsule (secondary cataract) with nanosecond Nd:YAG lasers (Aron-Rosa et al. 1980, Krasnov 1974).

### Refractive Surgery

At shorter pulse durations (1 ps–100 fs) and with lower energies, dielectric breakdown is applied to intrastromal dissection—formation of a corneal flap for refractive surgery (Kurtz et al. 1998)—as well as in cataract surgery (Palanker et al. 2010).

In addition to corneal reshaping, femtosecond lasers can produce an opaque plane in the corneal stroma with a small aperture on the optical axis, which limits the pupil size in order to extend the focal depth in patients with presbyopia. In this application, laser cuts a planar ring-shaped pocket in the cornea, where a dye is injected to produce a dark tattoo. This novel procedure can replace implantation of the small-aperture inlay (Lindstrom et al. 2013) for correction of presbyopia.

Another novel approach to refractive correction is based on adjustment of the corneal refractive index using molecular changes induced by multiphoton absorption of femtosecond laser in collagen (Ding et al. 2008). Although the changes in refractive index are rather small ( $5$  to  $15 \times 10^{-3}$ ), grating patterns were shown to produce diffractive lenses with 1.5–2 diopters of power. Such patterns in cat corneas have been shown to be stable for at least 12 months (Savage et al. 2014).

### Vitreoretinal Surgery

In addition to being tested in anterior chamber of the eye, ultrafast lasers have also been tested in the dissection of epiretinal membranes with a tightly focused beam (Cohen et al. 1997). Despite the very low energy requirements for this process (several microjoules with picosecond to femtosecond lasers), its applicability in the posterior pole is limited owing to the difficulty with axial discrimination between the epiretinal membranes and the retina located very close behind them. In addition, strong optical aberrations in the periphery of the posterior pole preclude tight focusing of the laser beam in these areas. However, further from the retina and from the posterior lens capsule, ultrafast lasers could be applied to dissection of the vitreous floaters (Gupta et al. 2003), especially if the pattern-scanning laser were guided by three-dimensional imaging to ensure safe separation from the surrounding tissues.

### Cataract Surgery

Cataract surgery is one of the most common surgical procedures in the United States, with approximately 2.5 million operations performed annually (Cent. Medicare Medicaid Serv. 2009). Lasers have long played an important role in the treatment of the posterior lens capsule opacification, called secondary cataract. Posterior capsule opacification occurs in approximately a third of the cases (Apple et al. 1992), and it was incised surgically for more than a century. Since 1974, the potential complications of bleeding and infection associated with such an open procedure

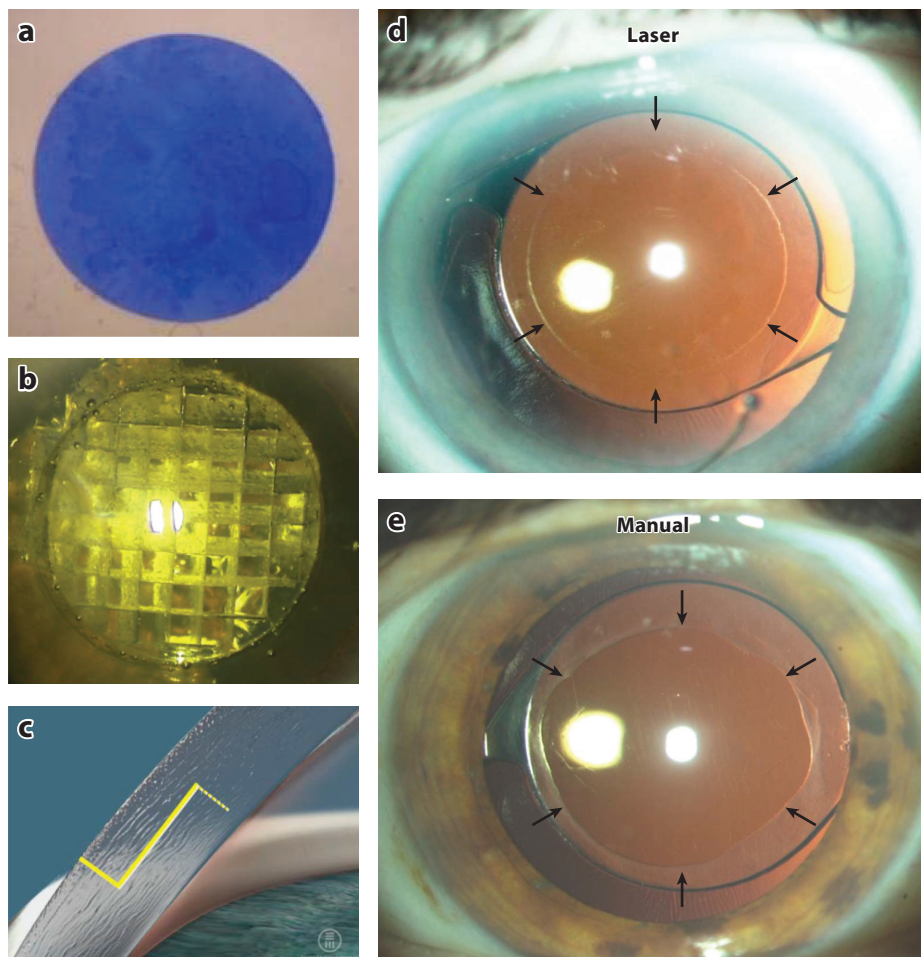


**Figure 9**

(a) A disk of the anterior capsule cut by laser during cataract surgery. (b) Crystalline lens segmented by femtosecond laser to ease its extraction during cataract surgery. (c) Multiplanar cut in the cornea produces the self-sealing incision, which reduces the fluid outflow during operation and prevents infections after cataract surgery. (d) An eye of a patient after the laser-assisted cataract surgery. Perfectly round edges of the laser capsulotomy are indicated by the arrows. (e) Patient's eye after conventional manual surgery, with very uneven capsulotomy pointed to by the arrows. Accurately shaped and centered capsulotomy helps ensure centration of the intraocular lens and perfect overlap of the capsule edges with the implant to prevent cellular proliferation into the posterior capsule, which leads to its opacification (secondary cataract). Adapted from Friedman et al. (2011).

have been avoided using the slit-lamp-coupled nanosecond Nd:YAG laser (Aron-Rosa et al. 1980, Krasnov 1974). Newer picosecond and femtosecond lasers have a lower threshold energy of dielectric breakdown, with accordingly reduced size of the cavitation bubble and associated tissue damage, and therefore allow more precise surgery.

Ultrashort-pulse lasers have been applied to softening of the aging crystalline lens in an attempt to restore accommodation. Initial attempts of generating intralenticular incisions to soften the lens tissue and reestablish its flexibility in presbyopia were performed with nanosecond laser

by Myers and Krueger (Krueger et al. 2001, Myers & Krueger 1998). Threshold energy and associated generation of the residual gas bubbles were later reduced with application of femtosecond pulses (Ripken et al. 2008). Recent investigations have shown softening of the crystalline lens by femtosecond laser (Hahn et al. 2015), and with properly selected laser settings, this process has not induced cataract formation (Krueger et al. 2012). Clinical trials are now in progress to assess the extent of improvement in accommodation in human patients undergoing laser lenticotomy.

Recently, a new laser-based technique was developed for anterior capsulotomy and lens segmentation (Nagy et al. 2009, Palanker et al. 2010). A scanning femtosecond laser can produce finely cut patterns in tissue, with their placement defined by integrated optical coherence tomography (OCT) imaging. Laser incisions in the anterior capsule are much more precise in size and shape than manual capsulorhexis (**Figure 9a,d,e**), ensuring perfect centration of the intraocular lens and accurate overlap of the capsular bag with the implant (Friedman et al. 2011). Segmentation and softening of the lens (**Figure 9b**) simplify its subsequent ultrasonic emulsification, thereby reducing the collateral damage to corneal endothelium during lens removal (Palanker et al. 2010). Femtosecond lasers have also been applied for construction of multiplanar self-sealing cataract incisions (**Figure 9c**) to improve safety of the procedure and prevent infections, and for exact placement of limbal relaxing incisions to reduce residual astigmatism (Palanker et al. 2010). Image-guided laser surgery eliminates the uncertainty of the surgical skills, tissue visibility, and variability of tissue elasticity and strength in various patients, making perfectly sized and centered cuts in every case. However, the large size of these laser systems precluded their integration into the surgical microscopes, and therefore laser dissection is performed as a separate procedure prior to cataract surgery. This additional step in cataract surgery slows the process and adds cost, thereby limiting the use of this technology in clinical practice. Smaller and less expensive lasers integrated into the surgical microscope would make this technology much more appealing and practical.

---

**Capsulotomy:**

circular cut in the anterior lens capsule to create an opening for removal of the crystalline lens and implantation of the intraocular lens

**Capsulorhexis:**

manual tearing of the anterior lens capsule in a circular pattern to create an opening for removal of the crystalline lens and implantation of the intraocular lens

---

## SUMMARY POINTS

1. Modern ophthalmic lasers enable unprecedented precision and selectivity in many therapeutic and surgical procedures and have become indispensable for ophthalmic care.
2. Progress in understanding of the laser–tissue interactions and the tissue response pathways leads to more selective and less damaging treatments, such as (*a*) minimally traumatic photocoagulation, which utilizes retinal plasticity to minimize scarring; (*b*) selective treatment of RPE and trabecular epithelium based on intracellular explosion of melanosomes using microsecond pulses; and (*c*) nondamaging laser therapy of the macula using transient hyperthermia below the damage threshold.
3. Advancements in laser and imaging technologies enable ultraprecise and fully automated surgery and therapy, such as refractive and cataract surgeries based on ultrafast lasers, or image-guided photocoagulation with eye tracking.

## FUTURE ISSUES

1. Variations of the retinal pigmentation as well as transparency of the ocular tissues and laser focusing affect the resulting temperature rise during treatment. Real-time dosimetry of the laser exposure on the retina or trabecular meshwork will ensure delivery of the desired dose in each spot, which is especially important for the nondamaging treatment.

2. As technology advances, manual treatments will be replaced with more automated pre-planned image-guided retinal laser therapy.
3. Large size and high cost of the ultrafast lasers preclude their penetration into clinical practice. Smaller and less expensive ultrafast lasers integrated with the surgical microscope in the operating room will allow broader use of this technology in cataract and refractive surgery.
4. Formation of transscleral channels with ultrafast near-infrared laser to allow controlled outflow of fluid from the eye for reduction of the intraocular pressure may replace more invasive manual glaucoma surgery.
5. Currently, there is no solution for the vitreous floaters—clumps of the vitreous gel, which may obscure parts of the visual field. Image-guided ablation of the vitreous floaters using ultrafast lasers may solve this problem.
6. Novel retinal therapies, such as NRT and SRT, will have to be validated in treatment of various macular disorders, including CSCR, MacTel, DME, and AMD.

## DISCLOSURE STATEMENT

The author is an inventor of the Pattern Scanning Laser Photocoagulator (PASCAL). The patent is licensed by Stanford University to Topcon Medical Laser Systems (TMLS). The author is also a consultant to TMLS. The author is an inventor of the OCT-guided femtosecond laser system for cataract surgery, which is manufactured by Abbott Medical Optics (AMO). The author is also a consultant to AMO.

## ACKNOWLEDGMENTS

I would like to thank Dr. Daniel Lavinsky from Federal University of Porto Alegre, Brazil, for providing the fundus image illustrating the effects of PRP and OCT images illustrating resolution of fluid in CSCR.

## LITERATURE CITED

- Apple DJ, Solomon KD, Tetz MR, Assia EI, Holland EY, et al. 1992. Posterior capsule opacification. *Surv. Ophthalmol.* 37:73–116
- Aron-Rosa D, Aron JJ, Griesemann M, Thyzel R. 1980. Use of the neodymium-YAG laser to open the posterior capsule after lens implant surgery: a preliminary report. *Am. Intraocul. Implant. Soc. J.* 6:352–54
- Barbu CE, Rasche W, Wiedemann P, Dawczynski J, Unterlauff JD. 2014. Pattern-Laser-Trabekuloplastik und Argon-Laser-Trabekuloplastik zur Glaukombehandlung [Pattern laser trabeculoplasty and argon laser trabeculoplasty for treatment of glaucoma]. *Ophthalmologe* 111:948–53
- Beckman H, Sugar HS. 1973. Laser iridectomy therapy of glaucoma. *Arch. Ophthalmol.* 90:453–55
- Beetham WP, Aiello LM, Balodimos MC, Koncz L. 1970. Ruby laser photocoagulation of early diabetic neovascular retinopathy: preliminary report of a long-term controlled study. *Arch. Ophthalmol.* 83:261–72
- Belokopytov M, Belkin M, Dubinsky G, Epstein Y, Rosner M. 2010. Development and recovery of laser-induced retinal lesion in rats. *Retina* 30:662–70
- Benner JD, Ahuja RM, Butler JW. 2002. Macular infarction after transpupillary thermotherapy for subfoveal choroidal neovascularization in age-related macular degeneration. *Am. J. Ophthalmol.* 134:765–68

- Blumenkranz MS, Yellachich D, Andersen DE, Wiltberger MW, Mordaunt D, et al. 2006. Semiautomated patterned scanning laser for retinal photocoagulation. *Retina* 26:370–76
- Bridges WB. 1964. Laser oscillation in singly ionized argon in visible spectrum (method: pulsed d-c discharge; transitions:  $4p \rightarrow 4s$ ,  $4p' \rightarrow 3d$ ; E). *Appl. Phys. Lett.* 4:128–30
- Brinkmann R, Hüttmann G, Rögner J, Roider J, Birngruber R, Lin CP. 2000. Origin of retinal pigment epithelium cell damage by pulsed laser irradiance in the nanosecond to microsecond time regimen. *Laser Surg. Med.* 27:451–64
- Brinkmann R, Roider J, Birngruber R. 2006. Selective retina therapy (SRT): a review on methods, techniques, preclinical and first clinical results. *Bull. Soc. Belge. Ophtalmol.* 302:51–69
- Brinkmann R, Schuele G, Joachimmeyer E, Roider J, Birngruber R. 2001. Determination of absolute fundus temperatures during retinal laser photocoagulation and selective RPE treatment. *Investig. Ophtalmol. Vis. Sci.* 42:S696
- Cent. Medicare Medicaid Serv. 2009. *Centers for Medicare & Medicaid Services Bulletin*, July 16, Baltimore, MD
- Cohen BZ, Wald KJ, Toyama K. 1997. Neodymium:YLF picosecond laser segmentation for retinal traction associated with proliferative diabetic retinopathy. *Am. J. Ophtalmol.* 123:515–23
- D'Amico DJ, Blumenkranz MS, Lavin MJ, Quiroz-Mercado H, Pallikaris IG, et al. 1996a. Multicenter clinical experience using an erbium:YAG laser for vitreoretinal surgery. *Ophtalmology* 103:1575–85
- D'Amico DJ, Brazitikos PD, Marcellino GR, Finn SM, Hobart JL. 1996b. Initial clinical experience with an erbium:YAG laser for vitreoretinal surgery. *Am. J. Ophtalmol.* 121:414–25
- Diabet. Retinopathy Study Res. Group. 1981. Photocoagulation treatment for proliferative diabetic retinopathy. Clinical application of Diabetic Retinopathy Study (DRS) findings, DRS report number 8. *Ophtalmology* 88:583–600
- Ding L, Knox WH, Bühren J, Nagy LJ, Huxlin KR. 2008. Intratissue refractive index shaping (IRIS) of the cornea and lens using a low-pulse-energy femtosecond laser oscillator. *Investig. Ophtalmol. Vis. Sci.* 49:5332–39
- Dorin G. 2004. Evolution of retinal laser therapy: minimum intensity photocoagulation (MIP). Can the laser heal the retina without harming it? *Semin. Ophtalmol.* 19:62–68
- Dougherty TJ, Mang TS. 1987. Characterization of intra-tumoral porphyrin following injection of hematoporphyrin derivative or its purified component. *Photochem. Photobiol.* 46:67–70
- Early Treat. Diabet. Retinopathy Study Res. Group. 1991. Early photocoagulation for diabetic retinopathy. ETDRS report number 9. *Ophtalmology* 98:766–85
- Elsner H, Pörksen E, Klatt C, Bunse A, Theisen-Kunde D, et al. 2006. Selective retina therapy in patients with central serous chorioretinopathy. *Graefes Arch. Clin. Exp. Ophtalmol.* 244:1638–45
- Ertan A, Bahadır M. 2006. Intrastromal ring segment insertion using a femtosecond laser to correct pellucid marginal corneal degeneration. *J. Cataract Refract. Surg.* 32:1710–16
- Figueira J, Khan J, Nunes S, Sivaprasad S, Rosa A, et al. 2009. Prospective randomised controlled trial comparing sub-threshold micropulse diode laser photocoagulation and conventional green laser for clinically significant diabetic macular oedema. *Br. J. Ophtalmol.* 93:1341–44
- Framme C, Alt C, Schnell S, Sherwood M, Brinkmann R, Lin CP. 2007. Selective targeting of the retinal pigment epithelium in rabbit eyes with a scanning laser beam. *Investig. Ophtalmol. Vis. Sci.* 48:1782–92
- Friedman NJ, Palanker DV, Schuele G, Andersen D, Marcellino G, et al. 2011. Femtosecond laser capsulotomy. *J. Cataract Refract. Surg.* 37:1189–98
- Garrison BJ, Srinivasan R. 1985. Laser ablation of organic polymers: microscopic models for photochemical and thermal processes. *J. Appl. Phys.* 57:2909–14
- Gass JD. 1971. Photocoagulation of macular lesions. *Trans. Am. Acad. Ophtalmol. Otolaryngol.* 75:580–608
- Glaucoma Laser Trial Res. Group. 1995. The Glaucoma Laser Trial (GLT) and Glaucoma Laser Trial Follow-Up Study: 7. Results. *Am. J. Ophtalmol.* 120:718–31
- Gupta R, Pannu BK, Bhargav S, Narang S, Sood S. 2003. Nd:YAG laser photostyotomy of a free-floating pigmented anterior vitreous cyst. *Ophtalmic Surg. Lasers Imaging* 34:203–5
- Hahn J, Fromm M, Al Halabi F, Besdo S, Lubatschowski H, et al. 2015. Measurement of ex vivo porcine lens shape during simulated accommodation, before and after fs-laser treatment. *Investig. Ophtalmol. Vis. Sci.* 56:5332–43

- Heisterkamp A, Mamom T, Drommer W, Ertmer W, Lubatschowski H. 2003. Photodisruption with ultra-short laser pulses for intrastromal refractive surgery. *Laser Phys.* 13:743–48
- Hemo I, Palanker D, Turovets I, Lewis A, Zauberman H. 1997. Vitreoretinal surgery assisted by the 193-nm excimer laser. *Investig. Ophthalmol. Vis. Sci.* 38:1825–29
- Isner J, Clarke R. 1987. The paradox of thermal ablation without thermal injury. *Laser Med. Sci.* 2:165–73
- Jain A, Blumenkranz MS, Paulus Y, Wiltberger MW, Andersen DE, et al. 2008. Effect of pulse duration on size and character of the lesion in retinal photocoagulation. *Arch. Ophthalmol.* 126:78–85
- Jonas JB. 2004. Corneal endothelial transplantation using femtosecond laser technology. *Eye* 18:657–58
- Kitai MS, Popkov VL, Semchishen VA, Kharizov AA. 1991. The physics of UV laser cornea ablation. *IEEE J. Quantum Elect.* 27:302–7
- Koinzer S, Baade A, Schlott K, Hesse C, Caliebe A, et al. 2015. Temperature-controlled retinal photocoagulation reliably generates uniform subvisible, mild, or moderate lesions. *Transl. Vis. Sci. Technol.* 4:9
- Koinzer S, Elsner H, Klatt C, Pörksen E, Brinkmann R, et al. 2008. Selective retina therapy (SRT) of chronic subfoveal fluid after surgery of rhegmatogenous retinal detachment: three case reports. *Graefes Arch. Clin. Exp. Ophthalmol.* 246:1373–78
- Kozak I, Oster SF, Cortes MA, Dowell D, Hartmann K, et al. 2011. Clinical evaluation and treatment accuracy in diabetic macular edema using navigated laser photocoagulator NAVILAS. *Ophthalmology* 118:1119–24
- Kramer M, Miller JW, Michaud N, Moulton RS, Hasan T, et al. 1996. Liposomal benzoporphyrin derivative verteporfin photodynamic therapy. Selective treatment of choroidal neovascularization in monkeys. *Ophthalmology* 103:427–38
- Krasnov MM. 1974. Q-switched laser goniopuncture. *Arch. Ophthalmol.* 92:37–41
- Krueger RR, Sun XK, Stroh J, Myers R. 2001. Experimental increase in accommodative potential after neodymium: yttrium-aluminum-garnet laser photodisruption of paired cadaver lenses. *Ophthalmology* 108:2122–29
- Krueger RR, Uy H, McDonald J, Edwards K. 2012. Ultrashort-pulse lasers treating the crystalline lens: Will they cause vision-threatening cataract? (An American Ophthalmological Society thesis). *Trans. Am. Ophthalmol. Soc.* 110:130–65
- Kurtz RM, Horvath C, Liu HH, Krueger RR, Juhasz T. 1998. Lamellar refractive surgery with scanned intrastromal picosecond and femtosecond laser pulses in animal eyes. *J. Refract. Surg.* 14:541–48
- Latina MA, Park C. 1995. Selective targeting of trabecular meshwork cells: in vitro studies of pulsed and CW laser interactions. *Exp. Eye Res.* 60:359–71
- Latina MA, Sibayan SA, Shin DH, Noecker RJ, Marcellino G. 1998. Q-switched 532-nm Nd:YAG laser trabeculoplasty (selective laser trabeculoplasty): a multicenter, pilot, clinical study. *Ophthalmology* 105:2082–88
- Lavinsky D, Cardillo JA, Melo LA Jr., Dare A, Farah ME, Belfort R Jr. 2011. Randomized clinical trial evaluating mETDRS versus normal or high-density micropulse photocoagulation for diabetic macular edema. *Investig. Ophthalmol. Vis. Sci.* 52:4314–23
- Lavinsky D, Palanker D. 2015. Nondamaging photothermal therapy for the retina: initial clinical experience with chronic central serous retinopathy. *Retina* 35:213–22
- Lavinsky D, Sramek C, Wang J, Huie P, Dalal R, et al. 2014. Subvisible retinal laser therapy: titration algorithm and tissue response. *Retina* 34:87–97
- Lavinsky D, Wang J, Huie P, Dalal R, Lee SJ, Lee DY, Palanker D. 2016. Nondamaging retinal laser therapy: rationale and applications to the macula. *Investig. Ophthalmol. Vis. Sci.* 57:2488–500
- L’Esperance FA Jr. 1968. An ophthalmic argon laser photocoagulation system: design, construction, and laboratory investigations. *Trans. Am. Ophthalmol. Soc.* 66:827–904
- L’Esperance FA Jr. 1969. The treatment of ophthalmic vascular disease by argon laser photocoagulation. *Trans. Am. Acad. Ophthalmol. Otolaryngol.* 73:1077–96
- Lindstrom RL, MacRae SM, Pepose JS, Hoopes PC Sr. 2013. Corneal inlays for presbyopia correction. *Curr. Opin. Ophthalmol.* 24:281–87
- Little HL, Zweng HC, Peabody RR. 1970. Argon laser slit-lamp retinal photocoagulation. *Trans. Am. Acad. Ophthalmol. Otolaryngol.* 74:85–97

- Luttrull JK, Sramek C, Palanker D, Spink CJ, Musch DC. 2012. Long-term safety, high-resolution imaging, and tissue temperature modeling of subvisible diode micropulse photocoagulation for retinovascular macular edema. *Retina* 32:375–86
- Maeshima K, Utsugi-Sutou N, Otani T, Kishi S. 2004. Progressive enlargement of scattered photocoagulation scars in diabetic retinopathy. *Retina* 24:507–11
- Maiman TH. 1960. Stimulated optical radiation in ruby. *Nature* 187:493–94
- Mainster MA, Reichel E. 2000. Transpupillary thermotherapy for age-related macular degeneration: long-pulse photocoagulation, apoptosis, and heat shock proteins. *Ophthalmic Surg. Lasers* 31:359–73
- Melamed S, Ben Simon GJ, Levkovitch-Verbin H. 2003. Selective laser trabeculoplasty as primary treatment for open-angle glaucoma: a prospective, nonrandomized pilot study. *Arch. Ophthalmol.* 121:957–60
- Merigan WH, Strazzeri J, DiLoreto DA Jr., Fischer W, Hunter JJ, et al. 2011. Visual recovery after outer retinal damage in the macaque. *Investig. Ophthalmol. Vis. Sci.* 52:3202
- Meyer-Schwickerath G. 1960. *Light Coagulation*. St. Louis, MO: Mosby
- Miller JW, Walsh AW, Kramer M, Hasan T, Michaud N, et al. 1995. Photodynamic therapy of experimental choroidal neovascularization using lipoprotein-delivered benzoporphyrin. *Arch. Ophthalmol.* 113:810–18
- Muqit MM, Marcellino GR, Gray JC, McLauchlan R, Henson DB, et al. 2010. Pain responses of Pascal 20 ms multi-spot and 100 ms single-spot panretinal photocoagulation: Manchester Pascal Study, MAPASS report 2. *Br. J. Ophthalmol.* 94:1493–98
- Myers RI, Krueger RR. 1998. Novel approaches to correction of presbyopia with laser modification of the crystalline lens. *J. Refract. Surg.* 14:136–39
- Nagar M, Ogunyomade A, O’Brart DP, Howes F, Marshall J. 2005. A randomised, prospective study comparing selective laser trabeculoplasty with latanoprost for the control of intraocular pressure in ocular hypertension and open angle glaucoma. *Br. J. Ophthalmol.* 89:1413–17
- Nagpal M, Marlecha S, Nagpal K. 2010. Comparison of laser photocoagulation for diabetic retinopathy using 532-nm standard laser versus multispot pattern scan laser. *Retina* 30:452–58
- Nagy Z, Takacs A, Filkorn T, Sarayba M. 2009. Initial clinical evaluation of an intraocular femtosecond laser in cataract surgery. *J. Refract. Surg.* 25:1053–60
- Newsom RSB, McAlister JC, Saeed M, McHugh JDA. 2001. Transpupillary thermotherapy (TTT) for the treatment of choroidal neovascularisation. *Br. J. Ophthalmol.* 85:173–78
- Niemz M. 2002. *Laser-Tissue Interactions. Fundamentals and Applications*. Berlin: Springer
- Nordan LT, Slade SG, Baker RN, Suarez C, Juhasz T, Kurtz R. 2003. Femtosecond laser flap creation for laser in situ keratomileusis: six-month follow-up of initial U.S. clinical series. *J. Refract. Surg.* 19:8–14
- Oh B-L, Yu HG. 2015. Choroidal thickness after full-fluence and half-fluence photodynamic therapy in chronic central serous chorioretinopathy. *Retina* 35:1555–60
- Palanker D, Hemo I, Turovets I, Zauberman H, Fish G, Lewis A. 1994. Vitreoretinal ablation with the 193-nm excimer laser in fluid media. *Investig. Ophthalmol. Vis. Sci.* 35:3835–40
- Palanker D, Lavinsky D, Blumenkranz MS, Marcellino G. 2011. The impact of pulse duration and burn grade on size of retinal photocoagulation lesion: implications for pattern density. *Retina* 31:1664–69
- Palanker DV, Blumenkranz MS, Andersen D, Wiltberger M, Marcellino G, et al. 2010. Femtosecond laser-assisted cataract surgery with integrated optical coherence tomography. *Sci. Transl. Med.* 2:58ra85
- Pallikaris IG, Papatzanaki ME, Siganos DS, Tsilimbaris MK. 1991. A corneal flap technique for laser in situ keratomileusis. Human studies. *Arch. Ophthalmol.* 109:1699–702
- Parodi MB, Spasse S, Iacono P, Di Stefano G, Canziani T, Ravalico G. 2006. Subthreshold grid laser treatment of macular edema secondary to branch retinal vein occlusion with micropulse infrared (810 nanometer) diode laser. *Ophthalmology* 113:2237–42
- Patz A, Maumenee AE, Ryan SJ. 1971. Argon laser photocoagulation. Advantages and limitations. *Trans. Am. Acad. Ophthalmol. Otolaryngol.* 75:569–79
- Paulus YM, Jain A, Gariano RF, Nomoto H, Schuele G, et al. 2010. Selective retinal therapy with a continuous line scanning laser. *Proc. SPIE 7550, San Francisco*. Bellingham, WA: SPIE
- Paulus YM, Jain A, Gariano RF, Stanzel BV, Marmor M, Blumenkranz MS, Palanker D. 2008. Healing of retinal photocoagulation lesions. *Investig. Ophthalmol. Vis. Sci.* 49:5540–45
- Pomerantzeff O, Lee PF, Hamada S, Donovan RH, Mukai N, Schepens CL. 1971. Clinical importance of wavelengths in photocoagulation. *Trans. Am. Acad. Ophthalmol. Otolaryngol.* 75:557–68

- Ratkay-Traub I, Juhasz T, Horvath C, Suarez C, Kiss K, et al. 2001. Ultra-short pulse (femtosecond) laser surgery: initial use in LASIK flap creation. *Ophthalmol. Clin. North Am.* 14:347–55
- Reichel E, Berrocal AM, Ip M, Kroll AJ, Desai V, et al. 1999. Transpupillary thermotherapy of occult subfoveal choroidal neovascularization in patients with age-related macular degeneration. *Ophthalmology* 106:1908–14
- Ripken T, Oberheide U, Fromm M, Schumacher S, Gerten G, Lubatschowski H. 2008. fs-Laser induced elasticity changes to improve presbyopic lens accommodation. *Graefes Arch. Clin. Exp. Ophthalmol.* 246:897–906
- Roider J, Hillenkamp F, Flotte T, Birngruber R. 1993. Microphotocoagulation: selective effects of repetitive short laser pulses. *PNAS* 90:8643–47
- Roider J, Michaud NA, Flotte TJ, Birngruber R. 1992. Response of the retinal pigment epithelium to selective photocoagulation. *Arch. Ophthalmol.* 110:1786–92
- Roisman L, Magalhaes FP, Lavinsky D, Moraes N, Hirai FE, et al. 2013. Micropulse diode laser treatment for chronic central serous chorioretinopathy: a randomized pilot trial. *Ophthalmic Surg. Lasers Imaging Retina* 44:465–70
- Savage DE, Brooks DR, DeMagistris M, Xu L, MacRae S, et al. 2014. First demonstration of ocular refractive change using blue-IRIS in live cats. *Investig. Ophthalmol. Vis. Sci.* 55:4603–12
- Schatz H, Madeira D, McDonald HR, Johnson RN. 1991. Progressive enlargement of laser scars following grid laser photocoagulation for diffuse diabetic macular edema. *Arch. Ophthalmol.* 109:1549–51
- Schmidt U, Birngruber R, Hasan T. 1992. [Selective occlusion of ocular neovascularization by photodynamic therapy]. *Ophthalmologe* 89:391–94
- Schmidt-Erfurth U, Hasan T, Gragoudas E, Michaud N, Flotte TJ, Birngruber R. 1994. Vascular targeting in photodynamic occlusion of subretinal vessels. *Ophthalmology* 101:1953–61
- Schuele G, Rumohr M, Huettmann G, Brinkmann R. 2005. RPE damage thresholds and mechanisms for laser exposure in the microsecond-to-millisecond time regimen. *Investig. Ophthalmol. Vis. Sci.* 46:714–19
- Schuele G, Huttmann G, Framme C, Roider J, Brinkmann R. 2004. Noninvasive optoacoustic temperature determination at the fundus of the eye during laser irradiation. *J. Biomed. Opt.* 9:173–79
- Sher A, Jones BW, Huie P, Paulus YM, Lavinsky D, et al. 2013. Restoration of retinal structure and function after selective photocoagulation. *J. Neurosci.* 33:6800–8
- Sivaprasad S, Elagouz M, McHugh D, Shona O, Dorin G. 2010. Micropulsed diode laser therapy: evolution and clinical applications. *Surv. Ophthalmol.* 55:516–30
- Sramek C, Mackanos M, Spittler R, Leung LS, Nomoto H, et al. 2011. Non-damaging retinal phototherapy: dynamic range of heat shock protein expression. *Investig. Ophthalmol. Vis. Sci.* 52:1780–87
- Sramek C, Paulus Y, Nomoto H, Huie P, Brown J, Palanker D. 2009. Dynamics of retinal photocoagulation and rupture. *J. Biomed. Opt.* 14:034007
- Sramek CK, Leung L-S, Paulus YM, Palanker DV. 2012. Therapeutic window of retinal photocoagulation with green (532-nm) and yellow (577-nm) lasers. *Ophthalmic Surg. Lasers Imaging* 4:341–47
- Srinivasan R, Leigh WJ. 1982. Ablative photodecomposition: action of far-ultraviolet (193 nm) laser radiation on poly(ethylene terephthalate) films. *J. Am. Chem. Soc.* 104:6784–85
- Srinivasan R, Wynne JJ, Blum SE. 1983. Far-UV photoetching of organic material. *Laser Focus* May:62–66
- Teichmann I, Teichmann KD, Fechner PU. 1976. Glaucoma operation with the argon laser. *Eye Ear Nose Throat Mon.* 55:58–62
- Telfair WB, Bekker C, Hoffman HJ, Yoder PR, Nordquist RE, et al. 2000. Histological comparison of corneal ablation with Er:YAG laser, Nd:YAG optical parametric oscillator, and excimer laser. *J. Refract. Surg.* 16:40–50
- Trokel SL, Srinivasan R, Braren B. 1983. Excimer laser-surgery of the cornea. *Am. J. Ophthalmol.* 96:710–15
- Turati M, Gil-Carrasco F, Morales A, Quiroz-Mercado H, Andersen D, et al. 2010. Patterned laser trabeculoplasty. *Ophthalmic Surg. Lasers Imaging* 41:538–45
- Venkatesh P, Ramanjulu R, Azad R, Vohra R, Garg S. 2011. Subthreshold micropulse diode laser and double frequency neodymium: YAG laser in treatment of diabetic macular edema: a prospective, randomized study using multifocal electroretinography. *Photomed. Laser Surg.* 29:727–33

- Verteporfin Photodyn. Ther. Study Group. 2001. Verteporfin therapy of subfoveal choroidal neovascularization in age-related macular degeneration: two-year results of a randomized clinical trial including lesions with occult with no classic choroidal neovascularization—verteporfin in photodynamic therapy report 2. *Am. J. Ophthalmol.* 131:541–60
- Vogel A, Venugopalan V. 2003. Mechanisms of pulsed laser ablation of biological tissues. *Chem. Rev.* 103:577–644
- Wise JB, Witter SL. 1979. Argon laser therapy for open-angle glaucoma. A pilot study. *Arch. Ophthalmol.* 97:319–22
- Woodburn KW, Engelman CJ, Blumenkranz MS. 2002. Photodynamic therapy for choroidal neovascularization: a review. *Retina* 22:391–405
- Wright CHG, Barrett SF, Ferguson RD, Rylander HG, Welch AJ. 2000. Initial in vivo results of a hybrid retinal photocoagulation system. *J. Biomed. Opt.* 5:56–61
- Writ. Comm. Diabet. Retinopathy Clinic. Res. Netw. 2007. Comparison of the modified Early Treatment Diabetic Retinopathy Study and mild macular grid laser photocoagulation strategies for diabetic macular edema. *Arch. Ophthalmol.* 125:469–80
- Young FR. 1989. *Cavitation*. Maidenhead, UK: McGraw-Hill Book Co.
- Zaret MM, Breinin GM, Schmidt H, Ripps H, Siegel IM, Solon LR. 1961. Ocular lesions produced by an optical maser (laser). *Science* 134:1525–26



# Contents

The Road to Certainty and Back <i>Gerald Westheimer</i> .....	1
Experience-Dependent Structural Plasticity in the Visual System <i>Kalen P. Berry and Elly Nedivi</i> .....	17
Strabismus and the Oculomotor System: Insights from Macaque Models <i>Vallabh E. Das</i> .....	37
Corollary Discharge and Oculomotor Proprioception: Cortical Mechanisms for Spatially Accurate Vision <i>Linus D. Sun and Michael E. Goldberg</i> .....	61
Mechanisms of Orientation Selectivity in the Primary Visual Cortex <i>Nicholas J. Priebe</i> .....	85
Perceptual Learning: Use-Dependent Cortical Plasticity <i>Wu Li</i> .....	109
Early Visual Cortex as a Multiscale Cognitive Blackboard <i>Pieter R. Roelfsema and Floris P. de Lange</i> .....	131
Ocular Photoreception for Circadian Rhythm Entrainment in Mammals <i>Russell N. Van Gelder and Ethan D. Buhner</i> .....	153
Probing Human Visual Deficits with Functional Magnetic Resonance Imaging <i>Stelios M. Smirnakis</i> .....	171
Retinoids and Retinal Diseases <i>Philip D. Kiser and Krzysztof Palczewski</i> .....	197
Understanding Glaucomatous Optic Neuropathy: The Synergy Between Clinical Observation and Investigation <i>Harry A. Quigley</i> .....	235
Vision and Aging <i>Cynthia Owsley</i> .....	255
Electrical Stimulation of the Retina to Produce Artificial Vision <i>James D. Weiland, Steven T. Walston, and Mark S. Humayun</i> .....	273

Evolution of Concepts and Technologies in Ophthalmic Laser Therapy <i>Daniel Palanker</i> .....	295
Low Vision and Plasticity: Implications for Rehabilitation <i>Gordon E. Legge and Susana T.L. Chung</i> .....	321
The Human Brain in Depth: How We See in 3D <i>Andrew E. Welchman</i> .....	345
Visual Object Recognition: Do We (Finally) Know More Now Than We Did? <i>Isabel Gauthier and Michael J. Tarr</i> .....	377
3D Displays <i>Martin S. Banks, David M. Hoffman, Joobwan Kim, and Gordon Wetzstein</i> .....	397
Capabilities and Limitations of Peripheral Vision <i>Ruth Rosenholtz</i> .....	437
Visual Confidence <i>Pascal Mamassian</i> .....	459

## Errata

An online log of corrections to *Annual Review of Vision Science* articles may be found at <http://www.annualreviews.org/errata/vision>